The conformation of NAD$^+$ bound to lactate dehydrogenase determined by nuclear magnetic resonance with suppression of spin diffusion

Sébastien J. F. Vincent*†, Catherine Zwahlen*†, Carol Beth Post‡, John W. Burgner§, and Geoffrey Bodenhausen*¶

*Center for Interdisciplinary Magnetic Resonance, National High Magnetic Field Laboratory, 1800 East Paul Dirac Drive, Tallahassee, FL 32310; ‡Department of Medicinal Chemistry, Purdue University, West Lafayette, IN 47907; and §Department of Biological Sciences, Purdue University, West Lafayette, IN 47907

ABSTRACT We have reinvestigated the conformation of NAD$^+$ bound to dogfish lactate dehydrogenase (LDH) by using an NMR experiment that allows one to exploit nuclear Overhauser effects to determine internuclear distances between pairs of protons, without perturbation of spin-diffusion effects from other protons belonging either to the cofactor or to the binding pocket of the enzyme. The analysis indicates that the structure of bound NAD$^+$ is in accord with the conformation determined in the solid state by x-ray diffraction for the adenosine moiety, but deviates significantly from that of the nicotinamide. The NMR data indicate conformational averaging about the glycosidic bond of the nicotinamide nucleotide. In view of the strict stereospecificity of catalysis by LDH and the conformational averaging of bound NAD$^+$ that we infer from solution-state NMR, we suggest that LDH binds the cofactor in both *syn* and *anti* conformations, but that binding interactions in the *syn* conformation are not catalytically productive.

In systems that can be crystalized, the conformation of substrates and cofactors bound to high molecular weight enzymes can be derived from x-ray diffraction studies. In cases where the exchange between the bound and free forms is fast, information from diffraction can be supplemented by solution-state one- or two-dimensional exchange transferred nuclear Overhauser effect spectroscopy (ET–NOESY) (1, 2). The transferred NOE method uses excess substrate or cofactor, so that the resonance lineshapes resemble those of the substrate or cofactor in free solution, whereas cross-relaxation or NOEs are predominantly determined by internuclear distances within the substrate or cofactor in the bound form. In applications to systems such as the cofactor NAD$^+$ in rapid exchange with dogfish lactate dehydrogenase (LDH) (3–5), it is usually assumed that ET–NOESY data can be interpreted on the assumption that, at least for short mixing times, spin-diffusion effects can be ignored. Spin diffusion occurs when the magnetization migrates through a set of nuclei in several consecutive steps, and can, in principle, be taken into account by the relaxation matrix method (6–12) provided all pathways can be measured. In this paper, it will be shown that spin-diffusion effects occur in the LDH·NAD$^+$ complex that involve not only protons belonging to the cofactor, but also protons belonging to the binding pocket of the enzyme. Such indirect processes cannot be analyzed properly by full relaxation matrix methods, because it is impossible to identify all protons in the enzyme pocket and their dipolar coupling partners. Nevertheless, these indirect relaxation pathways can be largely eliminated by an NMR experiment where spin diffusion is quenched (13–17). Other methods for suppressing spin diffusion (7, 18–23), or accounting for it in other ways (24, ‖) have been proposed. There are analogies between the approach discussed here with the situation that arises if all protons belonging to the binding pocket were replaced by deuterium, although there are some fundamental differences between the two approaches that will be discussed. The structural information derived from the cross-relaxation rates of nicotinamide proton pairs deviates from the structure obtained from x-ray crystallography. With the quenching of spin diffusion, the data strongly support conformational averaging about the glycosidic bond.

Theory. Cross-relaxation leads to a migration of longitudinal magnetization $\mathbf{M}_z(\tau_m)$, which can be described by solving a set of differential equations that can be traced back to Solomon (25–27):

$$\frac{d\Delta\mathbf{M}_z(\tau_m)}{dt} = \mathbf{L}\Delta\mathbf{M}_z(\tau_m), \qquad [1]$$

$$\Delta\mathbf{M}_z(\tau_m) = \exp\{\mathbf{L}\tau_m\}\Delta\mathbf{M}_z(\tau_m = 0)$$

$$= \left(1 + \mathbf{L}\tau_m + \frac{1}{2!}\mathbf{L}^2\tau_m^2 + ...\right)\Delta\mathbf{M}_z(\tau_m = 0), \qquad [2]$$

where τ_m is the mixing time of the ET–NOESY experiment, $\Delta\mathbf{M}_z(\tau_m)$ is a vector representing the deviations from equilibrium $\mathbf{M}_z(\tau_m) - \mathbf{M}_z^{eq}$ of the longitudinal magnetization components of N spins, and $\mathbf{L} = -\mathbf{R} + \mathbf{K}$ is comprised of the relaxation matrix $\mathbf{R}$ (with diagonal elements ρ_{ii} and off-diagonal elements σ_{ij}, which are proportional to r_{ij}^{-6}) and the exchange matrix $\mathbf{K}$. In simple cases, the expansion of Eq. **2** can be truncated to the term linear in τ_m for short mixing times, so that the structural information contained in the elements σ_{ij} of $\mathbf{L}$ can be retrieved by linear regression using the initial rate approximation. However, for systems such as the complex LDH·NAD$^+$ where the molecular mass is on the order of 140 kDa and the correlation time at least 60 ns, the quadratic term proportional to $\mathbf{L}^2\tau_m^2$ is important even for short mixing times (11, 28, 29). The spin-diffusion effects described by quadratic and higher order terms can lead to a blurring of the information about internuclear distances even for relatively short mixing times.

Molecular System. LDH catalyzes the reduction of pyruvate by NADH to form lactate and NAD^+. The transfer of a proton and two electrons (formally a hydride) from the nicotinamide ring of NADH to pyruvate happens with a nearly ideal stereospecificity (the error rate is estimated to be $< 10^{-9}$) (30). The catalytic step mediated by LDH is essential in the glycolysis part of the Cori cycle taking place in active skeletal muscles and erythrocytes. Because knowledge of the conformation of cofactors and substrates bound to enzymes is essential for understanding their function, and because the binding site for NAD^+ is similar in a variety of dehydrogenases such as skeletal muscle LDH, alcohol dehydrogenase, glyceraldehyde-3-phosphate dehydrogenase, and malate dehydrogenase, it is of interest to determine reliable geometric information about enzyme-cofactor complexes in solution. The NAD^+ binding region as determined by x-ray crystallography is made up of four α helices and six strands of parallel β sheets known as the Rossmann fold or dinucleotide binding domain. NAD^+ is bound in an extended conformation. The adenosine moiety in NAD^+ binds to a hydrophobic crevice, and the nicotinamide ring binds with the reactive side in a polar environment, whereas the other side of the nicotinamide ring faces hydrophobic residues.

MATERIALS AND METHODS

Purification of Dogfish LDH. LDH was purified from frozen muscle tissue of the Atlantic spiny dogfish, *Squalus acanthias*, using procedures described elsewhere (31, 32). The enzyme then was dialyzed against 99.9% D_2O containing 50 mM phosphate, pH 7.0. The final concentration of enzyme was adjusted to 17.5 mg/ml by adding dialysis buffer. Aliquots containing the appropriate concentration of NAD^+ cofactor (5 mM) were frozen by dropwize addition to liquid nitrogen. The frozen pellets were lyophilized for 24 h under vacuum produced by a mechanical pump. The samples were stored under dry nitrogen at $-20°C$. The samples were rehydrated by addition of 700 μl of 99.99% D_2O to a final concentration of $[LDH] \approx 0.5$ mM and $[NAD^+] \approx 5$ mM.

NMR Spectroscopy. The conventional NOESY experiment (33, 34) is modified (Fig. 1a) by inserting a doubly selective radio-frequency pulse in the middle of the mixing time τ_m to obtain the so-called QUIET-NOESY sequence (*q*uenching of *u*ndesirable *i*ndirect *e*xternal *t*rouble in NOESY) (13, 17). This allows one to invert two spectral regions selected to include the chemical shifts of a "source" and a "target" proton, which are chosen because their distance (i.e. their mutual cross-relaxation rate) is of strategic importance to resolve a confor-

mational ambiguity. An inversion pulse with the envelope of a Q^3 Gaussian cascade and a duration of 12 ms can be made doubly selective by placing the carrier frequency midway between the two chemical shifts and by modulating the amplitude with a function cos ω_at, where ω_a is equal to half the difference between the chemical shifts (13, 17). During the first half of the mixing time, the magnetization of the source spin migrates not only to the target spin, but also to other protons in the vicinity, including "indirect" protons H^i that belong to the binding pocket of the enzyme. The doubly selective inversion pulse changes the sign of the longitudinal magnetization components of both the source and target spins, so that their mutual Overhauser effect continues to build up during the second half of the mixing time. However, barring accidental degeneracy, the other (indirect) spins are not inverted by the doubly selective inversion pulse, and the flow of magnetization from the source to the indirect H^i spin in the first half of the mixing time is reversed in the second half. Likewise, the flow from H^i to the target spin is largely canceled. The net effect is that, to a good approximation, only direct cross-relaxation between the source and target spins will give rise to a cross-peak in ET–NOESY, and that contributions due to indirect H^i protons will be suppressed, provided the latter's magnetization components are not accidentally inverted by the doubly selective pulse. The effect bears some similarities, but is not identical, to what can be obtained by replacing all protons belonging to the binding pocket by deuterium nuclei[||]. In this case, one would not only expect to suppress the cross-relaxation rates σ_{ij} between cofactor protons and enzyme deuterons, but also to reduce the diagonal elements ρ_{ii} that describe the longitudinal self-relaxation of the cofactor protons in the Solomon equations (see Eq. **1**). The attenuation of self-relaxation represents an additional benefit of deuteration that cannot be obtained by simple manipulations of the magnetization. All experiments reported here were carried out on a Bruker DMX 300 system at 8°C. Build-up plots were recorded for $0 < \tau_m < 300$ ms. Complementary ET-NOESY experiments were carried out with a Varian Unity Plus 720 MHz spectrometer but are not shown here.

Data Processing. The data were processed using Bruker XWIN-NMR 1.1 software. Two-dimensional spectra were acquired with 12-ppm windows in both dimensions, 512 t_1-increments with 2,048 points each were recorded with 16 scans and a relaxation interval of 1 s. No zero-filling was used and window functions with $\pi/2$-shifted sine-bell in ω_1 and exponential multiplication in ω_2 with a line broadening of 2 Hz were applied before two-dimensional Fourier transformation. Baseline correction using a second-order polynomial function was applied to all spectra in both dimensions. Peak intensities were determined using the XWINNMR 1.1 integration module and used as input for a fitting program written in MATLAB (35) to carry out a linear regression with least-square fitting of cross-peak intensities (normalized by the corresponding diagonal peak intensities) as a function of the mixing time in the interval $0 < \tau_m < 100$ ms. Usually, it is not possible to derive accurate cross-relaxation rates from ET–NOESY data without using a full relaxation matrix analysis which takes into consideration the whole network of participating spins. In the LDH·NAD^+ complex this represents a particularly daunting problem due to the lack of information about the indirect protons belonging to the binding pocket and their dipolar couplings with the cofactor. In QUIET–ET–NOESY, however, spin diffusion is largely suppressed, so that this cumbersome approach is not necessary because the two spins of interest behave almost as an isolated two-spin system (36). We used the initial rate approximation (27, 37) for mixing times up to 100 ms.

X-Ray Distances. To identify protons belonging to the binding pocket that could mediate spin diffusion, we used the x-ray coordinates of a ternary complex of dogfish LDH with NADH and oxamate determined from diffraction data at 2.1 Å resolution (J. P. Griffith and M. G. Rossmann, Protein Data
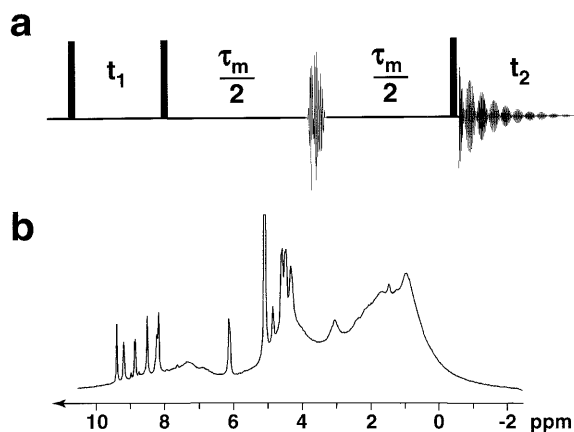

Fig. 1. (*a*) Pulse sequence used for the QUIET–ET–NOESY experiment where spin-diffusion pathways are quenched by doubly selective inversion of selected source and target protons. (*b*) One-dimensional spectrum of the LDH·NAD^+ complex in D_2O, with $[LDH] \approx 0.5$ mM, $[NAD^+] \approx 5$ mM, recorded at 8°C on a Bruker DMX 300 spectrometer, showing sharp resonances due to the cofactor and broad resonances due to the enzyme.

Bank file 1ldm). Oxamate was excluded, and the positions of the protons were determined based on geometry and optimal hydrogen bonding using the program CHARMM (38). The energy of the resulting structure was minimized to remove poor nonbonded interactions using parameters described previously (39), and 60 steps of the steepest descent algorithm with main-chain atoms harmonically constrained, followed by 100 steps of the conjugate gradient algorithm without constraints. All protons within a radius of 4.5 Å around the relevant NAD^+ protons were identified and taken into account in the following discussion.

RESULTS

The one-dimensional NMR spectrum shown in Fig. 1*b* of LDH and NAD^+ in excess with respect to LDH exhibits very broad lines from the enzyme, and some relatively sharp resonances resulting from the averaging of the signals of the free and bound forms of the cofactor. The conventional two-dimensional ET–NOESY spectrum in Fig. 2*a* shows cross-peaks between cofactor resonances that primarily reflect cross-relaxation processes in the bound form because those in the free form are negligible.
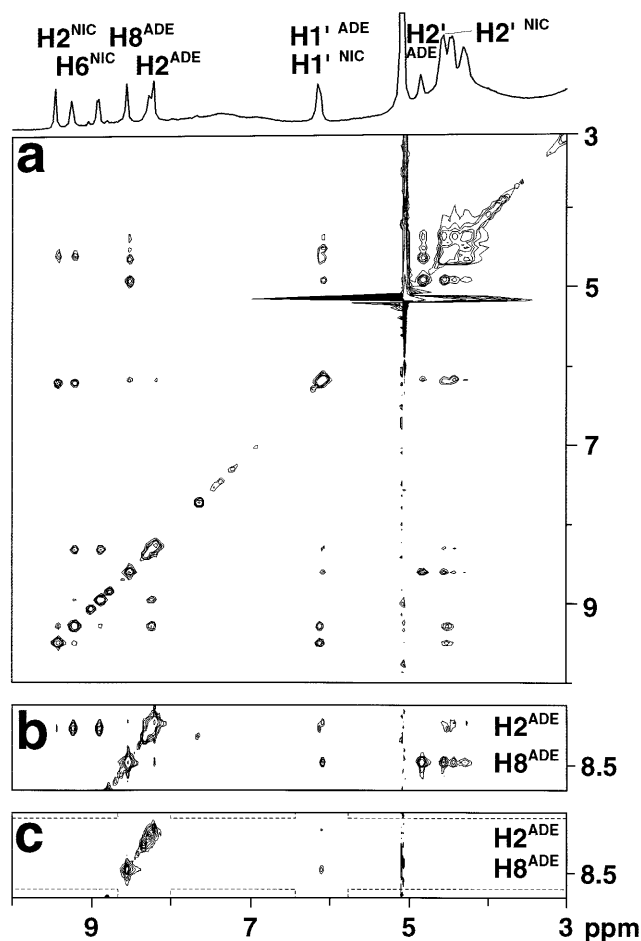

FIG. 2. (*a*) Conventional two-dimensional ET–NOESY of the LDH·NAD^+ complex, recorded with a mixing time τ_m = 150 ms. Relevant NAD^+ protons are labeled with ADE for adenosine and NIC for nicotinamide. (*b*) Strip from the ET-NOESY spectrum of *a* shown with lower contours. (*c*) Corresponding strip from a QUIET–ET–NOESY spectrum recorded under identical conditions. Doubly selective inversion was achieved by applying a 12-ms cosine-modulated Gaussian cascade Q^3 in the middle of the mixing time to invert two frequency bands (represented by dashed lines), each of ≈1.1 ppm width, centered around 6.07 ppm (to invert $H1'^{ADE}$ of the adenosine) and 8.36 ppm (to invert both adenosine protons $H2^{ADE}$ at 8.13 ppm and $H8^{ADE}$ at 8.47 ppm). No water suppression methods were used.

A direct two-spin interpretation of ET–NOESY intensities (Fig. 2 *a* and *b*) would indicate that, in the bound form, the aromatic $H2^{ADE}$ and $H8^{ADE}$ protons of the adenosine are at similar distances from the $H1'^{ADE}$ proton of the adenosine, an unreasonable conclusion given the structural constraints of adenosine nucleoside. The energy-minimized structure derived from x-ray diffraction (J. P. Griffith and M. G. Rossmann, Protein Data Bank file 1ldm) indicates an extended conformation of the cofactor within the binding pocket, as shown in Fig. 3, with distances of 4.6 Å ($H2^{ADE}$–$H1'^{ADE}$) and 3.9 Å ($H8^{ADE}$–$H1'^{ADE}$). The problem inherent to conventional NOE studies stems from the possibility that the magnetization is not transmitted directly from $H2^{ADE}$ (or $H8^{ADE}$) to $H1'^{ADE}$, but first from $H2^{ADE}$ (or $H8^{ADE}$) to one or several unknown protons H^i that belong to the binding site of LDH, and from there to the $H1'^{ADE}$ proton of the adenosine. To resolve the ambiguity, we measured cross-peak intensities as a function of mixing time using the method discussed above that effectively restricts cross-relaxation to a pair of spins. In the case of the LDH·NAD^+ complex, the $H1'^{ADE}$ proton was taken to be the source spin, and the $H2^{ADE}$ and $H8^{ADE}$ protons were both target spins (Figs. 2*c* and 4*a*). The two telltale cross-peaks at ω_2 = 6.07 ppm ($H1'^{ADE}$) show a different behavior when spin diffusion is quenched: the peak correlating $H2^{ADE}$ and $H1'^{ADE}$ is strongly attenuated in the modified experiment, thus indicating that the corresponding peak in conventional ET–NOESY (Fig. 2*b*) must be due primarily to spin diffusion. Thus, the cross-relaxation rate between $H2^{ADE}$ and $H1'^{ADE}$ tends to be overestimated in ET–NOESY, so that the distance between these protons will be underestimated. For cross-relaxation between $H1'^{ADE}$ and $H2^{ADE}$, there are several protons belonging to the LDH binding pocket that may be involved in the flow of magnetization. The energy-minimized proton coordinates derived from diffraction data indicate that the protons H^α(Gly27), H^α(Asp52), and the methyl protons of Val53 and Ala96 all should lie in the proximity of $H2^{ADE}$ and $H1'^{ADE}$ of the adenosine moiety (Fig. 5*a*). Although their identity can be inferred from the x-ray structure, the protons belonging to the binding pocket of a large enzyme cannot be probed by magnetic resonance because of their line widths, and therefore cannot be taken into account in a full relaxation matrix analysis. Nonetheless, their contributions to spin diffusion are suppressed in the QUIET–ET–NOESY experiment of Fig. 2*c*, because their chemical shifts do not lie within one of the inverted regions. In contrast to $H2^{ADE}$, the intensity of the cross-peak between $H8^{ADE}$ and $H1'^{ADE}$ is hardly attenuated when spin diffusion is suppressed (Fig. 4*a*), which indicates a direct NOE between these two spins. In the bound form, the adenosine $H8^{ADE}$ or $H1'^{ADE}$ proton are far (>3.9 Å) from any other proton except the adenosine $H2'^{ADE}$.
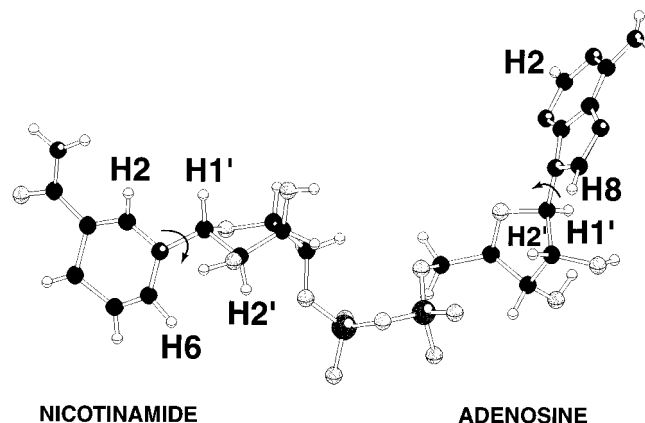

FIG. 3. Structure of NAD^+ in the binding pocket of LDH as derived from x-ray diffraction, obtained from Protein Data Bank file No. 1ldm.

The orientation of the nicotinamide ring with respect to the neighboring ribose is relevant to the understanding of LDH catalytic activity. In this case, the aromatic nicotinamide proton H2^{NIC} (or H6^{NIC}) can be chosen as the source spin and the H1$'^{NIC}$ (or H2$'^{NIC}$) ribose proton as the target. For the cross-relaxation processes H2^{NIC} → H1$'^{NIC}$ and H6^{NIC} → H1$'^{NIC}$, the suppression of spin diffusion by QUIET–ET–NOESY has little effect (Fig. 4*b*), indicating that these two cross-peak intensities are primarily due to direct Overhauser effects. However, the build-up between H6^{NIC} and H1$'^{NIC}$ is too rapid for protons that should be separated by 3.7 Å if the x-ray structure is relevant, whereas that between H2^{NIC} and H1$'^{NIC}$ is too weak for a distance of 2.4 Å. In contrast to the NOEs observed on H1$'^{NIC}$, cross-relaxation between H2$'^{NIC}$ and either H2^{NIC} or H6^{NIC} is attenuated when diffusion is quenched in the QUIET–ET–NOESY experiment (Fig. 4*c*), thus hinting at the existence of protons that are close enough to mediate spin diffusion. The x-ray structure suggests that H1$'^{NIC}$, H6^{NIC}, and H$^{\beta'}$(Asn138) might be responsible for spin diffusion in the case H2^{NIC} → H2$'^{NIC}$ (Fig. 5*c*). The magnetization transfer H6^{NIC} → H2$'^{NIC}$ is also significantly attenuated by quenching spin diffusion, although this cannot be explained by the x-ray structure because a distance between H6^{NIC} and H2$'^{NIC}$ of only 2.1 Å is so short that spin diffusion is unlikely to interfere. In addition, the NOE between H6^{NIC} and H2$'^{NIC}$ is smaller than that between H2^{NIC} and H2$'^{NIC}$. A possible resolution to the enigmatic relaxation behavior of the nicotinamide nucleotide is presented in *Discussion*.

Further experiments were developed to attempt the identification of protons belonging to the binding pocket that could
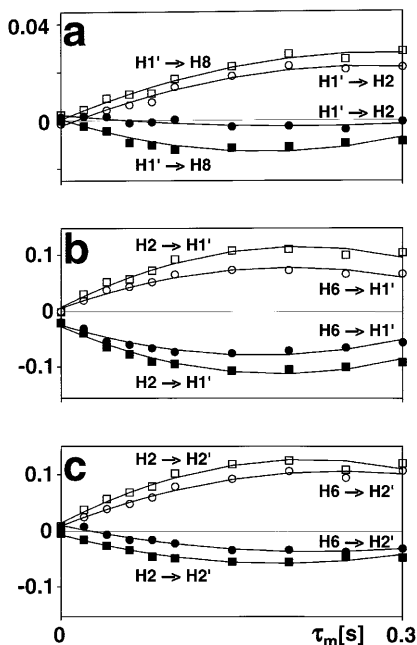

FIG. 4.   Build-up curves obtained by recording spectra at different mixing times. Conventional ET–NOESY amplitudes, which are positive, are represented by open circles and squares, while QUIET–ET–NOESY amplitudes, which are negative because of the inversion in the middle of the mixing time, are represented by filled symbols. The cross-peak amplitudes were normalized with respect to the diagonal peaks. The initial slopes were determined by linear fitting, and polynomials were used only for graphical purposes. (*a*) Cross-relaxation from adenosine ribose H1$'^{ADE}$ to adenosine H8^{ADE} (squares) and from H1$'^{ADE}$ to adenosine H2^{ADE} (circles). The latter build-up is strongly attenuated when spin diffusion is suppressed. (*b*) Cross-relaxation from nicotinamide H2^{NIC} to ribose H1$'^{NIC}$ (squares) and from H6^{NIC} to H1$'^{NIC}$ (circles). (*c*) Cross-relaxation from nicotinamide H2^{NIC} to ribose H2$'^{NIC}$ (squares) and from H6^{NIC} to H2$'^{NIC}$ (circles).
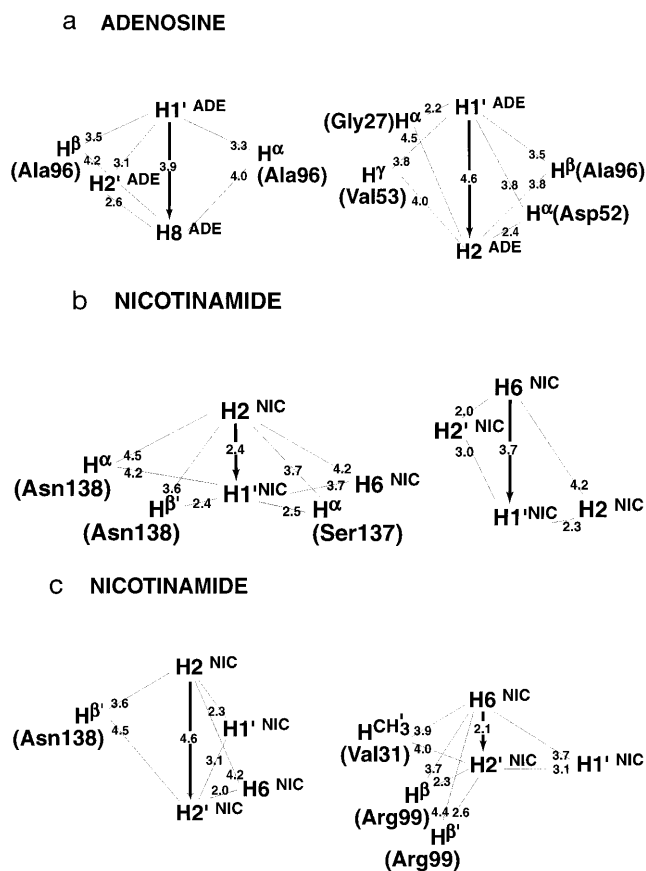

FIG. 5.   Representation of the x-ray distances between spins that are relevant to the cases studied in Fig. 4 *a–c*. All distances are drawn to scale.

be responsible for spin diffusion. In principle, contributions to ET–NOESY cross-peaks involving aliphatic protons of the enzyme can be suppressed in an experiment using a band-selective pulse instead of the doubly selective pulse of Fig. 1*a*. In this context, "aliphatic" stands for all protons with resonances below 4 ppm, which can be inverted in the middle of the mixing time by a band-selective inversion pulse applied at −0.3 ppm with a bandwidth of about 2,400 Hz (8 ppm at 300 MHz). This can be achieved by using a Q^3 pulse (13, 40–42) with a duration of 2 ms, which should be reasonably effective even if the T$_2$s of the LDH protons are very short. In this experiment (data not shown), the peak intensities remained the same as in conventional ET–NOESY. We therefore may conclude tentatively that the protons of the LDH binding pocket that mediate spin diffusion between NAD$^+$ protons do not resonate below 4 ppm. This excludes a participation of the H$^{\gamma}$(Val53) and H$^{\beta}$(Ala96) protons in the cross-relaxation between H1$'^{ADE}$ and H2^{ADE} in the adenosine moiety (Fig. 5*a*), although the x-ray distances would seem to make these protons possible candidates. It is possible that H$^{\gamma}$(Val53) and H$^{\beta}$(Ala96) do not participate actively because they cross-relax rapidly with other spins within the enzyme. Similarly, H$^{\gamma}$(Val31), H$^{\beta'}$(Arg99) and H$^{\beta'}$(Asn138) can be excluded from playing a role in spin diffusion. These conclusions appear to be compatible with the x-ray structure. On the other hand, the negative outcome of the experiment with band-selective inversion of all aliphatic protons does not allow one to exclude H$^{\alpha}$(Gly27) and H$^{\alpha}$(Asp52), which are likely to resonate above 4 ppm, from playing a role in spin diffusion between H1$'^{ADE}$ and H2^{ADE} (Fig. 5*a*). In general, the band-selective inversion experiment does not allow one to exclude any backbone H$^{\alpha}$, any aromatic protons, or, if the studies are carried out in light water, any amide protons.

Biophysics: Vincent *et al.*

Proc. Natl. Acad. Sci. USA 94 (1997)   4387

By extracting cross-relaxation rates from the initial slope of the cross-peak intensities as a function of the mixing time for experiments where spin-diffusion is quenched (filled symbols in Fig. 4), assuming negligible contributions from free NAD^+, and assuming that the local correlation times are the same for the two internuclear vectors, we can estimate the ratio of the distances according to:

$$\frac{r_{ij}}{r_{kl}} = \left(\frac{\sigma_{kl}}{\sigma_{ij}} \right)^{\frac{1}{6}}. \qquad [3]$$

The observed averaged σ_{kl} values should be almost equal to the true cross-relaxation rates in the bound form scaled by the molar fraction of bound form (2, 11). The scaling factor cancels in the ratio of Eq. **3**, so that this ratio appears to be a good approximation in all examples discussed, because we are concerned with interactions between a ribose proton and an aromatic proton.

DISCUSSION

The effects of spin diffusion are evident when comparing intensities in conventional ET–NOESY and QUIET–ET–NOESY. Examination of Fig. 4 shows that the initial slopes of the NOE build-up curves are significantly smaller in QUIET–ET–NOESY in 3 of 6 cases (adenosine H1'^{ADE}–H2^{ADE}; nicotinamide H2'^{NIC}–H2^{NIC}, and H2'^{NIC}–H6^{NIC}). That the intensities in conventional ET–NOESY are boosted by spin diffusion must be attributed to the presence of one or several "indirect" protons that are closer to the "directly" involved protons than the latter are to each other. In systems undergoing exchange, the enhancement by an indirect proton is significantly greater if the latter belongs to the enzyme than if it belongs to the cofactor, assuming a similar spatial arrangement (11). Thus, an indirect NOE enhancement via *inter*molecular relaxation pathways is more effective than via *intra*molecular pathways within the cofactor when the latter can shuttle back and forth between free and bound states. Magnetization that migrates to an "indirect" proton belonging to the cofactor tends to dissipate during the time spent in the free state, where cross-relaxation is negligible, but longitudinal relaxation still effective. Note that in Fig. 4, the initial slopes in QUIET–ET–NOESY never appear to be greater than those in ET–NOESY. Indeed, for cases where interactions to many neighboring spins act as a "relaxation sink" and therefore attenuate direct NOEs, the results of QUIET–ET-NOESY would be expected to be similar to those of conventional ET–NOESY, because inversion pulses do not alter the self-relaxation rates.

Adenosine Base-Ribose Interactions. For the proton pairs of the adenosine base, the differences between QUIET–ET–NOESY and conventional ET–NOESY can be readily interpreted with reference to the crystallographic structure of an LDH complex. For the adenosine proton pair H1'^{ADE}–H8^{ADE}, both experiments give comparable initial slopes, indicating negligible contributions from spin diffusion. This proton pair is separated by as much as 3.9 Å in the x-ray structure, but there are no LDH protons that are close enough to both H1'^{ADE} and H8^{ADE} (i.e. < 3.9 Å) to enhance their NOE intensity. The possibility of two-step transfer processes within the cofactor is suggested by the presence of two cross-peaks in conventional ET–NOESY (Fig. 2a) that correlate H1'^{ADE} and H8^{ADE} with H2'^{ADE}. However, intramolecular cross-relaxation is less efficient, and spin diffusion mediated by the H2'^{ADE} proton is weak, given the outcome of the QUIET–ET–NOESY experiment. On the other hand, a significant spin-diffusion contribution is observed for the adenosine pair H1'^{ADE}–H2^{ADE} (Fig. 4a). In the crystal structure of an LDH complex, H$^\alpha$(Gly27), H$^\alpha$(Asp52) and the methyl protons of Val53 and Ala96 are nearer to both H1'^{ADE} and H2^{ADE} than the direct distance of 4.6 Å between them (Fig. 5a). The negative result of the band-selective inversion experiment allows one to exclude the methyl protons and indicates that H$^\alpha$(Gly27) and H$^\alpha$(Asp52) must be primarily responsible for the indirect contributions to the

cross-peak between H1'^{ADE} and H2^{ADE}. The QUIET–ET–NOESY experiment of Fig. 1a should quench the effects of all four hypothetical indirect pathways between H1'^{ADE} and H2^{ADE}, because the chemical shifts of H$^\alpha$(Gly27), H$^\alpha$(Asp52), and the methyl protons of Val53 and Ala96 are not likely to lie within the inverted frequency bands. Even if one of the invisible protons accidentally had a shift lying within an inverted frequency band, the doubly selective pulse of 12 ms duration would fail to invert this enzyme proton effectively because of its rapid transverse relaxation. If we assume for simplicity that such a proton would be saturated rather than inverted, simulations indicate that its contribution to spin diffusion would be roughly reduced to one-half (data not shown). Therefore, the cross-relaxation rates of the proton pairs H1'^{ADE}–H2^{ADE} and H1'^{ADE}–H8^{ADE} measured by QUIET–ET–NOESY can be considered to be reliable.

Nicotinamide Base–Ribose Interactions. In contrast to the adenosine proton pairs, the NOE results for the nicotinamide proton pairs cannot be easily rationalized with reference to the crystallographic structure. It is difficult to account for both the importance of the indirect contributions evident by comparing conventional ET–NOESY and QUIET–ET–NOESY results, and the relative magnitudes of the QUIET–ET–NOESY cross-peaks. One does not expect any significant effect of quenching on the cross-peak intensity H2'^{NIC}–H6^{NIC} considering the interproton distances in the x-ray structure. The NOE intensity arising from this short-distance interaction (2.1 Å) would not be expected to be boosted by spin diffusion because the likelihood of finding intermediate protons at shorter distances is small. Yet, the QUIET–ET–NOESY build-up curve for this spin pair is attenuated to a degree similar to that observed for other interactions, of much larger separation, between a ribose proton and a nicotinamide base proton such as H2'^{NIC}–H2^{NIC} (4.6 Å, Fig. 4c). With regard to NOE magnitudes, neither H2^{NIC} → H1'^{NIC} nor H6^{NIC} → H2'^{NIC} yield intensities that are large enough (compared with those of the adenosine interactions, Fig. 4a) to be consistent with the short distances observed in the crystal. This point is further discussed below. Moreover, the NOE build-up for H6^{NIC} → H2'^{NIC} is slower than that for H2^{NIC} → H2'^{NIC}, in contradiction to the relative intensities expected for distances of 2.1 Å and 4.6 Å, respectively. A satisfactory interpretation of these data requires a more elaborate model than a single structure.

It would not be prudent to attempt to extract absolute internuclear distances from the cross-relaxation rates derived from these experiments. In such a large system with an overall correlation time of about 60 ns, internal motions must affect various internuclear vectors differently, so that it is not sufficient to describe the fluctuations of the dipole-dipole interactions by a single correlation time. However, it appears reasonable to estimate relative distances using Eq. **3**, because all pairs considered

Table 1. Comparison of ratios of internuclear distances (r) in NAD^+ bound in LDH pocket

Ratio	X-ray*	QUIET-ET-NOESY	ET-NOESY
		Adenosine	
$\dfrac{r(\text{H1'}^{ADE}\text{–H2}^{ADE})}{r(\text{H1'}^{ADE}\text{–H8}^{ADE})}$	1.18	1.21	1.15
		Nicotinamide	
$\dfrac{r(\text{H1'}^{NIC}\text{–H6}^{NIC})}{r(\text{H1'}^{NIC}\text{–H2}^{NIC})}$	1.61	1.02	1.02
$\dfrac{r(\text{H2'}^{NIC}\text{–H2}^{NIC})}{r(\text{H2'}^{NIC}\text{–H6}^{NIC})}$	2.19	0.96	0.93
$\dfrac{r(\text{H1'}^{NIC}\text{–H6}^{NIC})}{r(\text{H2'}^{NIC}\text{–H6}^{NIC})}$	1.76	0.95	1.05

*Ratios deduced from the energy-minimized x-ray structure.

consist of one ribose proton and one aromatic proton on the neighboring ring. The relative distances determined in this work are given in Table 1, together with relative distances derived from x-ray diffraction. A notable feature of Table 1 is that most of the ratios listed for nicotinamide are in the vicinity of one. Thus both $H2^{NIC}$ and $H6^{NIC}$ would appear to be nearly equidistant from $H1'^{NIC}$ and from $H2'^{NIC}$. Examination of the structure of NAD^+ in Fig. 3 shows that such constraints cannot be satisfied with a single conformation. A conformation that allows $H2^{NIC}$ to be equidistant from $H1'^{NIC}$ and $H2'^{NIC}$ cannot simultaneously account for $H6^{NIC}$ being equidistant from the same two ribose protons. Moreover, any single low-energy rotamer would place either $H2^{NIC}$ or $H6^{NIC}$ at a short distance (say 2.5 Å) to one of the ribose protons, which should give rise to a significantly greater NOE intensity than is measured for the adenosine pair $H1'^{ADE}$–$H8^{ADE}$ (distance about 3.9 Å.) If we consider the ratio $(3.9 \text{ Å}/2.5 \text{ Å})^6$, one would expect the initial slope of one of the cross-peaks of the nicotinamide moiety to be approximately 14-fold steeper than for the $H1'^{ADE}$–$H8^{ADE}$ cross-peak. In the actual QUIET–ET–NOESY experiment, only a 4-fold steeper slope was observed. This discrepancy is too large to be accounted for by spurious effects of diagonal elements ρ_{ii} of the relaxation matrix, or by residual spin-diffusion effects, e.g., by contributions from indirect spins that accidentally resonate within the doubly selective inversion windows. A more likely interpretation of the data suggests motional averaging, in such a manner that the apparent distances are nearly equivalent. One possibility would be that the NAD^+ cofactor can bind LDH with the nicotinamide base in both *syn* and *anti*. Other models of conformational averaging also may be consistent with the ratios in Table 1. Studies of other dehydrogenases suggest that the dinucleotide binding site of the Rossmann fold does not rigidly restrain the nicotinamide ring. Crystallographic studies at 1.9 Å resolution of malate dehydrogenase (MDH) show a weak density around the nicotinamide ring in a difference map calculated from a binary MDH-citrate complex and a ternary MDH–NAD–citrate complex (43). Conformational averaging, among other factors, could give rise to such a weak electron density. A study of glutamate dehydrogenase provides another clue: the possibility of mixed binding modes of the nicotinamide ring of $NADP^+$ in the complex with glutamate dehydrogenase was suggested by Banerjee and co-workers (44), although effects of spin diffusion and nonselective irradiation in their one-dimensional ET–NOE experiments were not taken into account. If the results reported here, which are free from spin-diffusion effects, are combined with an evaluation of conformational averaging by a complete relaxation matrix analysis, they should allow one to obtain a more elaborate assessment of the conformational equilibrium of NAD^+ binding to LDH than was previously possible.

Conformational Averaging and Hydride Transfer. The catalysis of hydride transfer by LDH is stereospecific for the A-side hydrogen of nicotinamide by more than a factor of 10^9 (30). The spatial arrangement of the cofactor and substrate and the preference for A-side transfer are consistent with binding the *anti* form of NAD^+. Binding *syn* NAD^+ with the same spatial arrangement would imply transfer of the B-side hydrogen. Assuming that the conformational averaging involves a combination of *syn* and *anti* forms, how can this be consistent with the stereospecificity for the A-side hydrogen? One explanation is that multiple binding modes of nicotinamide are not possible in the ternary complex. LDH is known to bind cofactor and substrate sequentially, and the substrate may dock only if the cofactor is bound in the *anti* form. However, if multiple binding modes are also possible in the ternary complex, one must conclude that hydride transfer cannot take place in the *syn* conformation. Although B-side dehydrogenase clearly demonstrates that B-side transfer using *syn*-NAD^+ is chemically feasible in specific cases, only A-side transfer from the *anti* conformation is productive in

the case of LDH, where catalysis requires very precise binding interactions in the active site.

The interpretation of QUIET–ET–NOESY data recorded under conditions where spin diffusion is suppressed is more straightforward than for conventional ET–NOESY data. A simplified analysis using Eq. 3 is thus legitimate and allows one to extract accurate relative internuclear distances. This approach should find applications in many structural studies.

1. Bothner-By, A. A. & Gassend, R. (1972) *Ann. N.Y. Acad. Sci.* **222,** 668–676.
2. Rosevear, P. R. & Mildvan, A. S. (1989) *Methods Enzymol.* **177,** 333–357.
3. Holbrook, J. J., Liljas, A., Steindel, S. J. & Rossmann, M. G. (1975) in *The Enzymes,* ed., Boyer, P. D. (Academic, New York), Vol. XI, pp. 191–292.
4. White, J. L., Hackert, M. L., Buehner, M., Adams, M. J., Ford, G. C., Lentz, P. J., Jr., Smiley, I. E., Steindel, S. J. & Rossmann, M. G. (1976) *J. Mol. Biol.* **102,** 759–779.
5. Abad-Zapatero, C., Griffith, J. P., Sussman, J. L. & Rossmann, M. G. (1987) *J. Mol. Biol.* **198,** 445–467.
6. Dobson, C. M., Olejniczak, E. T., Poulsen, F. M. & Ratcliffe, R. G. (1982) *J. Magn. Reson.* **48,** 97–110.
7. Olejniczak, E. T., Gampe, R. T., Jr., & Fesik, S. W. (1986) *J. Magn. Reson.* **67,** 28–41.
8. Boelens, R., Koning, T. M. G. & Kaptein, R. (1988) *J. Mol. Struct.* **173,** 299–311.
9. Borgias, B. A. & James, T. L. (1988) *J. Magn. Reson.* **79,** 493–512.
10. Post, C. B., Meadows, R. P. & Gorenstein, D. G. (1990) *J. Am. Chem. Soc.* **112,** 6796–6803.
11. Zheng, J. & Post, C. B. (1993) *J. Magn. Reson. B* **101,** 262–270.
12. Ni, F. (1994) *Progr. NMR Spectroc.* **26,** 517–606.
13. Zwahlen, C., Vincent, S. J. F., Di Bari, L., Levitt, M. H. & Bodenhausen, G. (1994) *J. Am. Chem. Soc.* **116,** 362–368.
14. Levitt, M. H. & Di Bari, L. (1992) *Phys. Rev. Lett.* **69,** 3124–3127.
15. Levitt, M. H. & Di Bari, L. (1994) *Bull. Magn. Reson.* **16,** 94–114.
16. Vincent, S. J. F., Zwahlen, C., Bolton, P. H., Logan, T. M. & Bodenhausen, G. (1996) *J. Am. Chem. Soc.* **118,** 3531–3532.
17. Vincent, S. J. F., Zwahlen, C. & Bodenhausen, G. (1996) *J. Biomol. NMR* **7,** 169–172.
18. Massefski, W., Jr. & Redfield, A. G. (1988) *J. Magn. Reson.* **78,** 150–155.
19. Fejzo, J., Krezel, A. M., Westler, W. M., Macura, S. & Markley, J. L. (1991) *J. Magn. Reson.* **92,** 651–657.
20. Burghardt, I, Konrat, R., Boulat, B., Vincent, S. J. F. & Bodenhausen, G. (1993) *J. Chem. Phys.* **98,** 1721–1736.
21. Boulat, B., Burghardt, I. & Bodenhausen, G. (1992) *J. Am. Chem. Soc.* **114,** 10679.
22. Hoogstraten, C. G., Westler, W. M., Macura, S. & Markley, J. L. (1993) *J. Magn. Reson. B* **102,** 232–235.
23. Zolnai, Z., Juranic, N., Markley, J. L. & Macura, S. (1995) *Chem. Phys.* **200,** 161–179.
24. Zheng, J. & Post, C. B. (1996) *J. Phys. Chem.* **100,** 2675–2680.
25. Solomon, I. (1955) *Phys. Rev.* **99,** 559–565.
26. Ernst, R. R., Bodenhausen, G. & Wokaun, A. (1987) *Principles of Nuclear Magnetic Resonance in One- and Two-Dimensions* (Clarendon, Oxford).
27. Neuhaus, D. & Williamson, M. (1989) *The Nuclear Overhauser Effect in Structural and Conformational Analysis* (VCH, New York).
28. Kalk, A. & Berendsen, H. J. C. (1976) *J. Magn. Reson.* **24,** 343–366.
29. Lane, A. N. (1988) *J. Magn. Reson.* **78,** 425–439.
30. LaReau, R. D. & Anderson, V. E. (1992) *Biochem.* **31,** 4174–4180.
31. Burgner, J. W., II, & Ray, W. J., Jr. (1974) *Biochem.* **13,** 4229–4237.
32. Burgner, J. W., II, & Ray, W. J., Jr. (1978) *Biochem.* **17,** 1654–1661.
33. Meier, B. H. & Ernst, R. R. (1979) *J. Am. Chem. Soc.* **101,** 6441–6442.
34. Anil Kumar, Ernst, R. R. & Wüthrich, K. (1980) *Biochem. Biophys. Res. Commun.* **95,** 1–6.
35. MATLAB (Copyright 1984–1994) (The Mathworks Company, Inc.), Version 4.2a.
36. Schwager, M. & Bodenhausen, G. (1996) *J. Magn. Reson. Ser. B* **111,** 40–49.
37. Olejniczak, E. T., Poulsen, F. M. & Dobson, C. M. (1981) *J. Am. Chem. Soc.* **103,** 6574–6580.
38. Brooks, B. R., Brucoleri, R. E., Olafson, B. D., Slater, D. J., Swaminathan, S. & Karplus, M. (1983) *J. Comput. Chem.* **4,** 187–217.
39. Young, L. & Post, C. B. (1993) *J. Am. Chem. Soc.* **115,** 1964–1970.
40. Emsley, L., Burghardt, I. & Bodenhausen, G. (1990) *J. Magn. Reson.* **90,** 214–220.
41. Emsley, L., Burghardt, I. & Bodenhausen, G. (1991) *J. Magn. Reson.* **94,** 448.
42. Emsley, L. & Bodenhausen, G. (1992) *J. Magn. Reson.* **97,** 135–148.
43. Hall, M. D. & Banaszak, L. J. (1993) *J. Mol. Biol.* **232,** 213–233.
44. Banerjee, S., Levy, H. R., Levy, G. C., Limuti, C., Goldstein, B. M. & Bell, J. E. (1987) *Biochemistry* **26,** 8443–8450.